doi:10.1038/nature09413

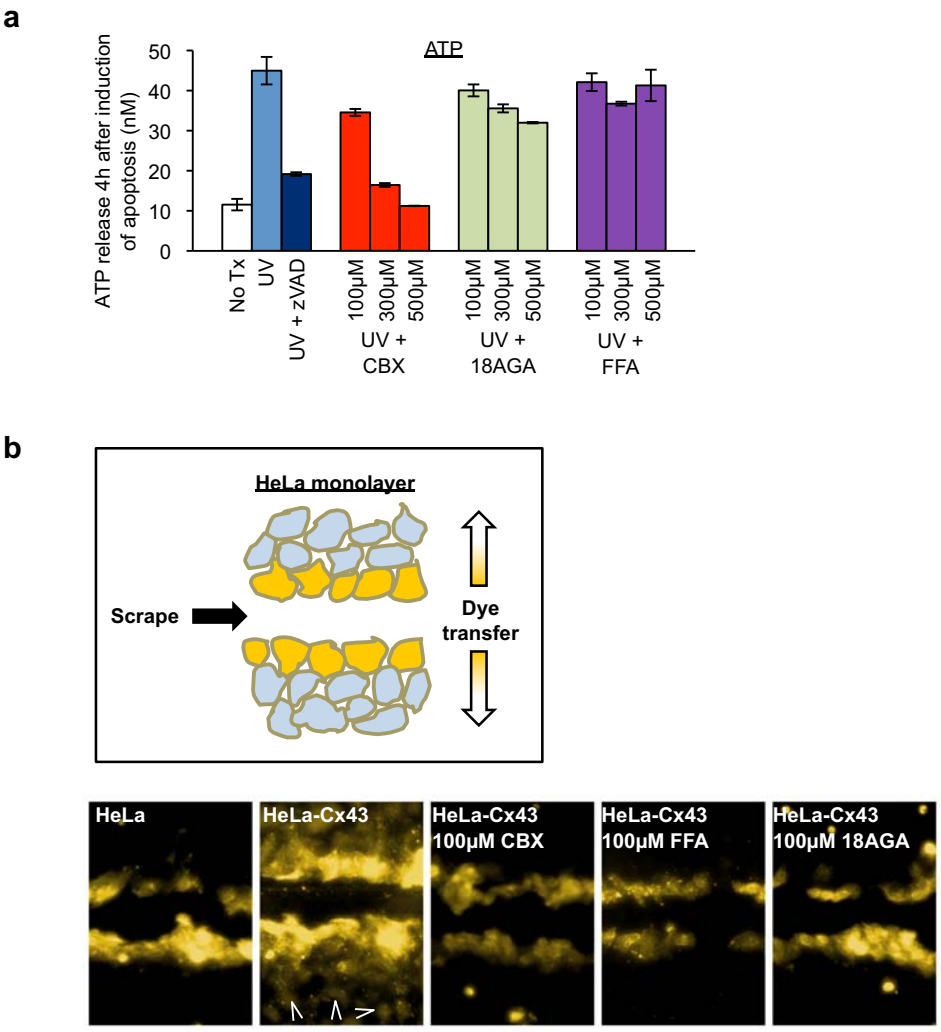

Supplementary Figure 1. Release of ATP during apoptosis is sensitive to carbenoxolone. **a,** ATP concentrations in Jurkat cell supernatants 4h after apoptosis induction under the indicated treatments. Error bars, s.d.; *n* = 2. **b,** (Top) Schematic depicting scrape assay to determine connexin-mediated gap junction activity. Monolayer of cells are scraped and cells adjacent to scrape are damaged and take up the dye Lucifer Yellow added to the medium. Dye is then transferred to neighboring cells through gap junctions. HeLa Cells stably expressing the gap junction protein Connexin 43 (Cx43) and the control cells not expressing Cx43 were used in this assay. (Bottom) Transfer of Lucifer Yellow in the scrape assay performed with HeLa cells, demonstrating that gap junction inhibitors FFA and 18AGA are functional in this assay (although these drugs did not affect find-me signal release from apoptotic cells). All drugs are used at 100μM.

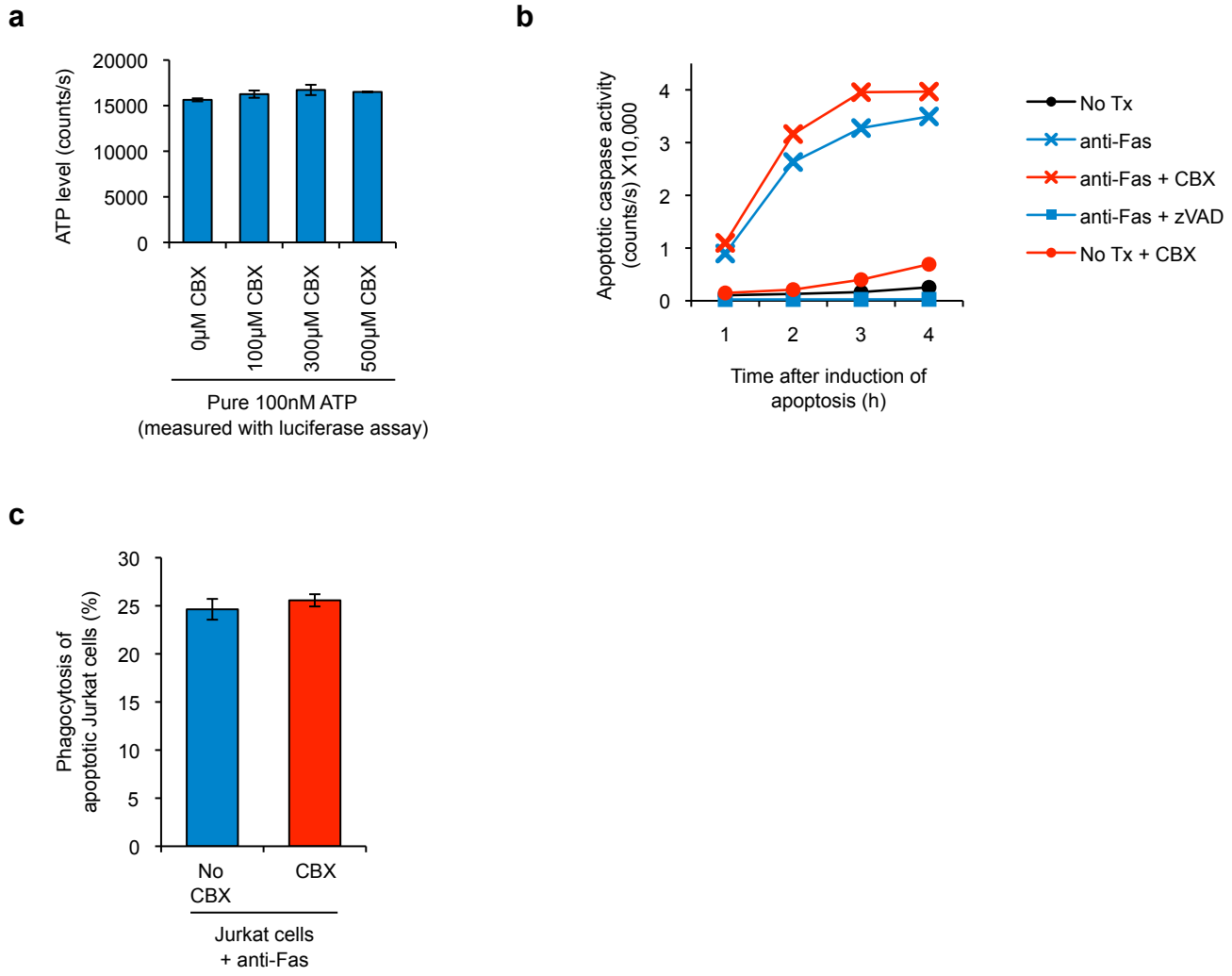

Supplementary Figure 2. Carbenoxolone does not interfere with the ATP assay, and does not inhibit the progression of apoptosis.

a, ATP quantification assay (luciferase/luciferin) performed in the presence of varying concentrations of CBX, demonstrating that CBX does not affect the ATP assay. Assay performed in triplicate. Error bars, s.d. Data representative of two independent experiments. **b,** CBX does not inhibit the apoptotic process. Apoptotic caspase activity was assessed in Jurkat cells either untreated or induced to undergo apoptosis under the conditions indicated. CBX was used at 500μM and zVAD at 100μM. **c,** CBX, while inhibiting nucleotide find-me signal release, does not affect exposure of eat-me signals. CBX-treated (and TAMRA-labeled) apoptotic Jurkat cells, when mixed together with bone marrow derived macrophages, were recognized and phagocytosed as determined by this engulfment assay. Since CBX (500μM) was also present throughout the engulfment assay, this suggests that CBX did not affect the ability of macrophages to recognize or engulf apoptotic cells. Error bars, s.d.; representative of two independent experiments.

a

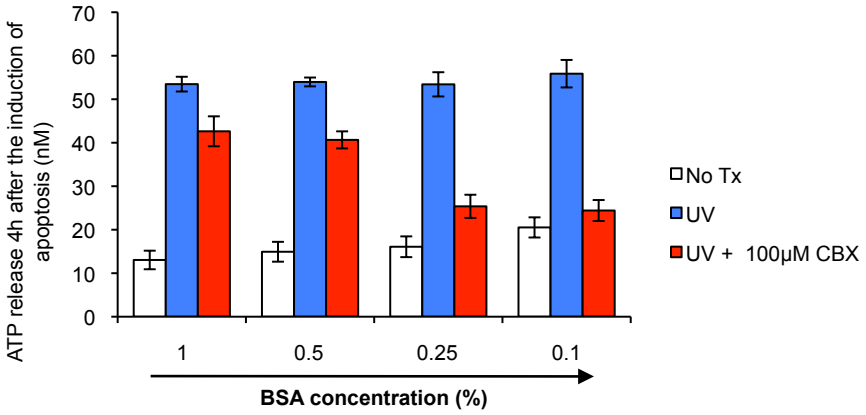

b

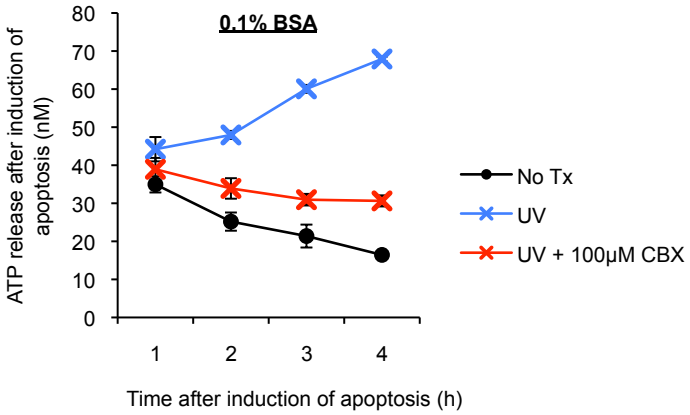

Supplementary Figure 3. Carbenoxolone is more efficacious at lower BSA concentrations. **a,** Efficacy of CBX is decreased in the presence of BSA. Jurkat cells were induced to undergo apoptosis in the presence or absence of 100μM CBX in media with different concentrations of BSA. Supernatants were collected after 4h and the levels of ATP assessed. CBX inhibition of ATP release from apoptotic cells increases as BSA concentration decreases. This provided an explanation for the need to use higher concentrations of CBX to see better inhibition in our experiments (presented in **Supplementary Fig. S1a**). Error bars, s.e.m.; *n* = 3. **b,** Time course of ATP release performed in lower BSA concentration (0.1%) demonstrates that lower CBX concentration (100μM) is effective at blocking ATP release. The first time point (1h) also demonstrates that resuspending the cells in the lower BSA concentration results in a high basal ATP concentration, possibly due to hypoosmotic stimulation of the cells. Error bars, s.e.m.; *n* = 3.

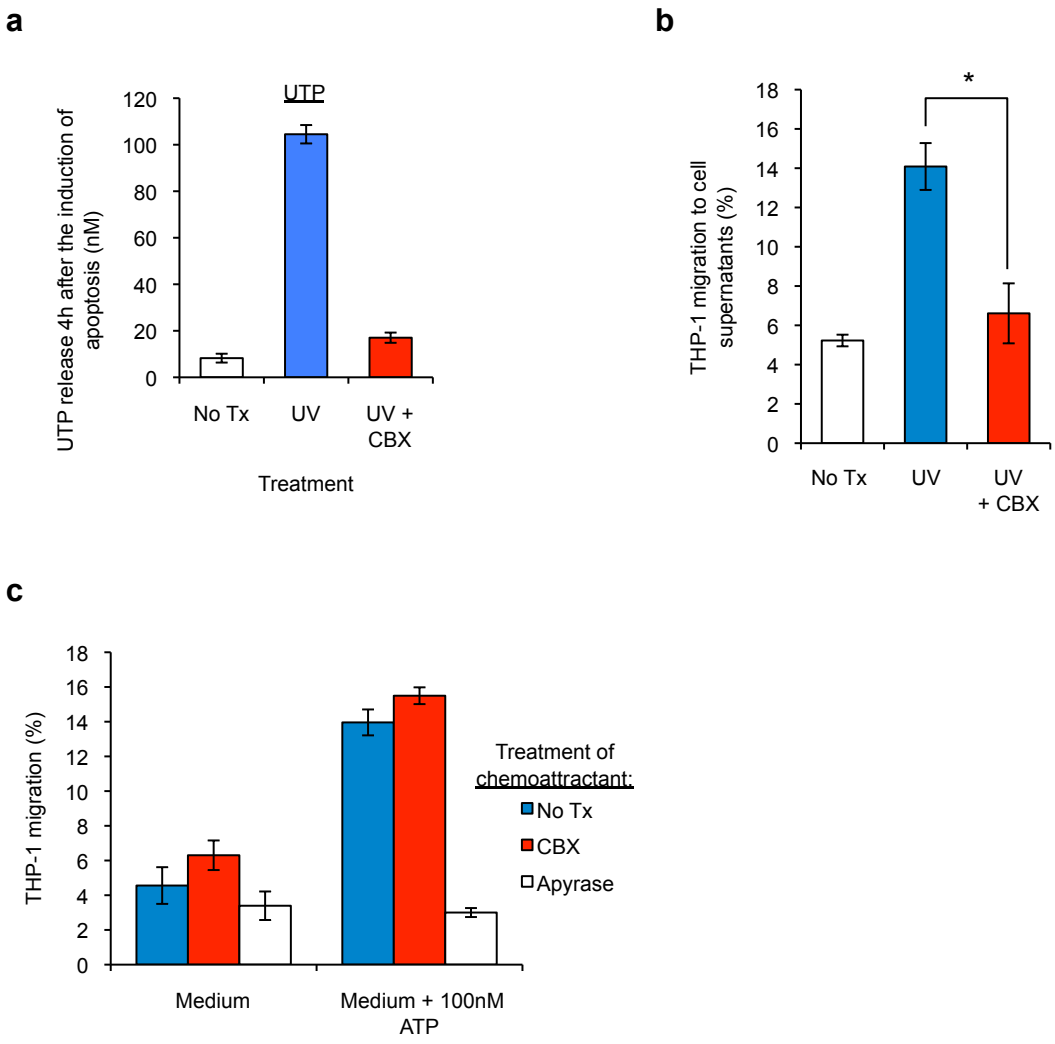

Supplementary Figure 4. Carbenoxolone blocks the release of find-me signals from apoptotic cells.

a, CBX (500μM) also blocks the release of UTP from apoptotic cells. UTP levels in Jurkat cell supernatants were measured 4h after induction of apoptosis. Error bars, s.e.m.; *n* = 3. **b,** CBX (500μM) inhibits the release of find-me signal from apoptotic cells. Migration of THP-1 monocytes toward apoptotic cell supernatants was performed using 1:4 dilutions of supernatants collected from Jurkat cells 4h after apoptosis induction. Error bars, s.d.; $P < 0.05$. Data are representative of 2 independent experiments. **c,** CBX does not directly affect migration of monocytes to nucleotides. Migration of THP-1 cells to medium containing purified nucleotides, treated with 500μM CBX (which does not affect migration) or apyrase (used as a positive control for inhibition of migration by degrading the nucleotides/chemoattractant). Error bars, s.d.

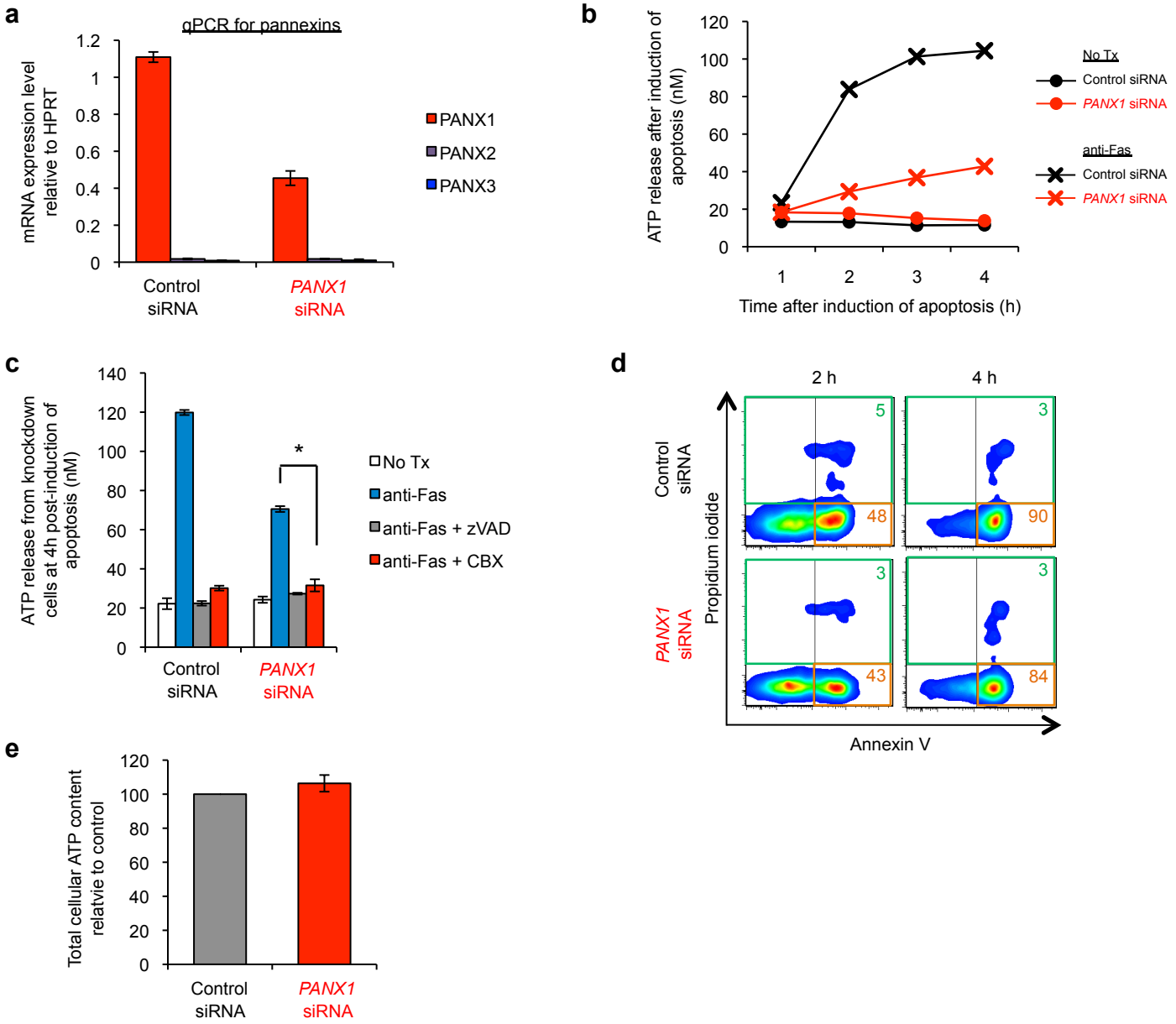

Supplementary Figure 5. Pannexin 1 knockdown reduces ATP release without inhibiting apoptosis or decreasing total intracellular ATP content.

a, Quantitative PCR demonstrates that knockdown of PANX1 does not result in upregulation of *PANX2* or *PANX3* mRNA. Error bars, s.d.; *n* = 2. **b,** Time course of ATP release from control and PANX1 siRNA-transfected cells induced to undergo Fas-mediated apoptosis. Representative of 2 independent experiments. **c,** Residual ATP release from *PANX1*-siRNA-transfected apoptotic Jurkat cells is sensitive to caspase inhibition and CBX treatment. zVAD (50μM) and CBX (500μM) were added to Jurkat cells transfected with control siRNA or *PANX1* siRNA, and the ATP release from cells 4h after anti-Fas mediated apoptosis was assessed. Error bars, s.e.m.; $P < 0.005$, $n = 3$. **d,** Control and *PANX1* siRNA treated Jurkat cells undergo comparable apoptosis at 2 and 4h time points, as assessed by exposure of phosphatidylserine detected via annexin V staining (*x* axis) and exclusion of propidium iodide (*y* axis). Propidium iodide (PI) staining revealed low percentages of necrotic cells under these conditions (PI positive). Percentage of 'apoptotic' (orange; $AnxV^+PI^-$) and 'necrotic' (green; PI^+) cells are shown on graphs. **e,** Total intracellular ATP in siRNA transfected cells normalized to control siRNA cells. Error bars, s.e.m.; *n* = 3.

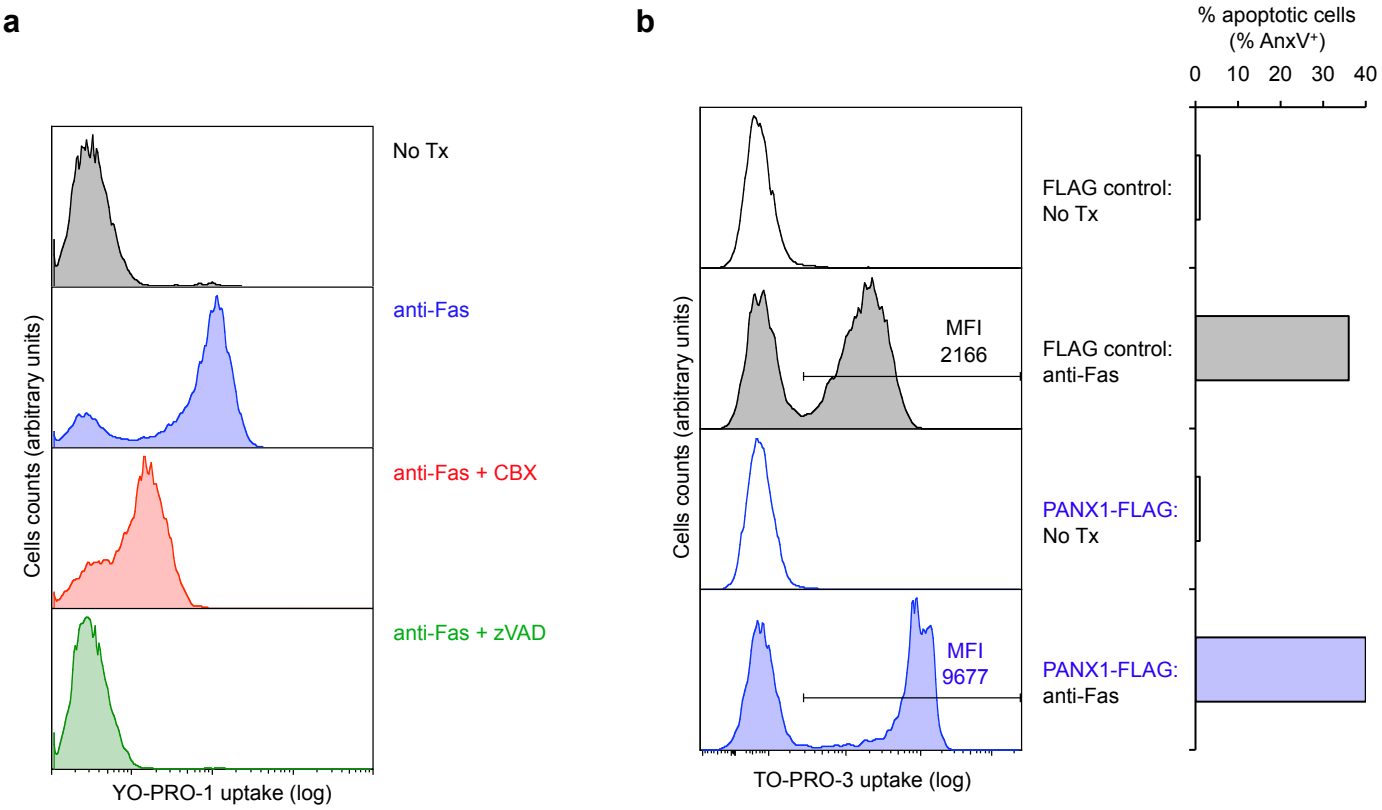

Supplementary Figure 6. Pannexin 1 mediates the uptake of apoptotic cell indicator dyes. **a,** CBX treatment significantly inhibits YO-PRO-1 uptake by apoptotic Jurkat cells. Flow cytometry histograms show YO-PRO-1 uptake by Jurkat cells 4h after the induction of apoptosis, in the absence or presence of zVAD (50μM) or CBX (500μM). **b,** Transient expression of PANX1-FLAG boosts TO-PRO-3 uptake by apoptotic Jurkat cells. Jurkat cells were transiently transfected with plasmids encoding mCherry (as a marker of transfection) along with either control FLAG tag or PANX1-FLAG. (Left) Flow cytometry histogram profiles show TO-PRO-3 uptake by mCherry^{high} populations, from the control and PANX1-FLAG transfected cells, induced to undergo apoptosis. MFI for TO-PRO-3^{+}-gated population is shown to indicate the increased TO-PRO-3 uptake due to PANX1-FLAG expression. (Right) The bar graph shows the percentage of apoptotic cells (% annexin V^{+}) in the entire population.

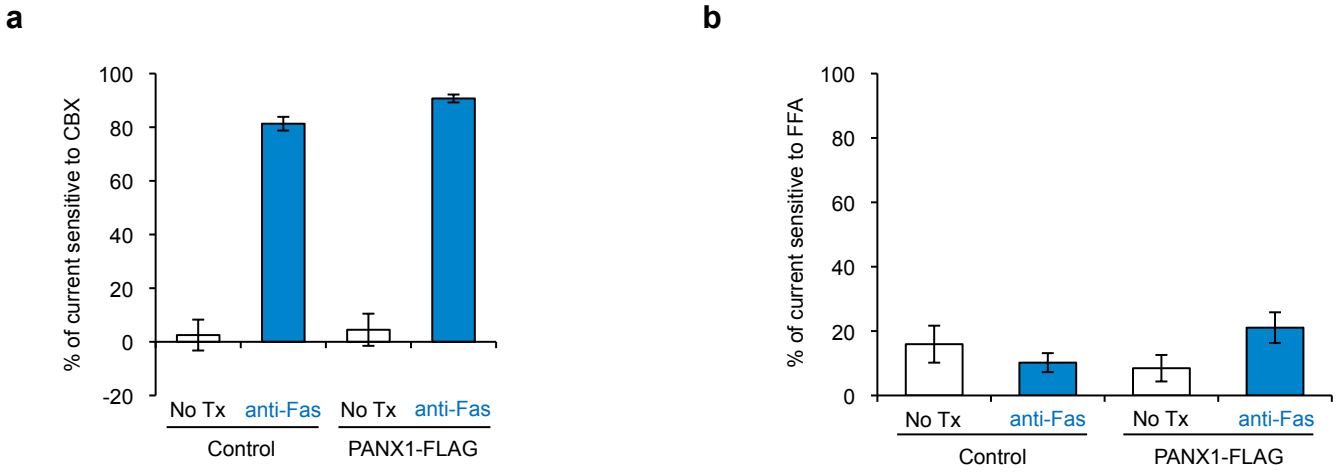

Supplementary Figure 7. Patch-clamp analysis demonstrates that apoptosis-induced plasma membrane currents are sensitive to carbenoxolone and not flufenamic acid.
Percentage of peak current that is sensitive to 100μM CBX (**a**) or 100μM FFA (**b**) in control and PANX1-FLAG stable cell lines. Please note that only 'dying' (blebbing) cells were included in the analyses of the anti-Fas treatment groups. Error bars, s.e.m.; $n \geq 7$ (**a**) or 4 (**b**) for each group.

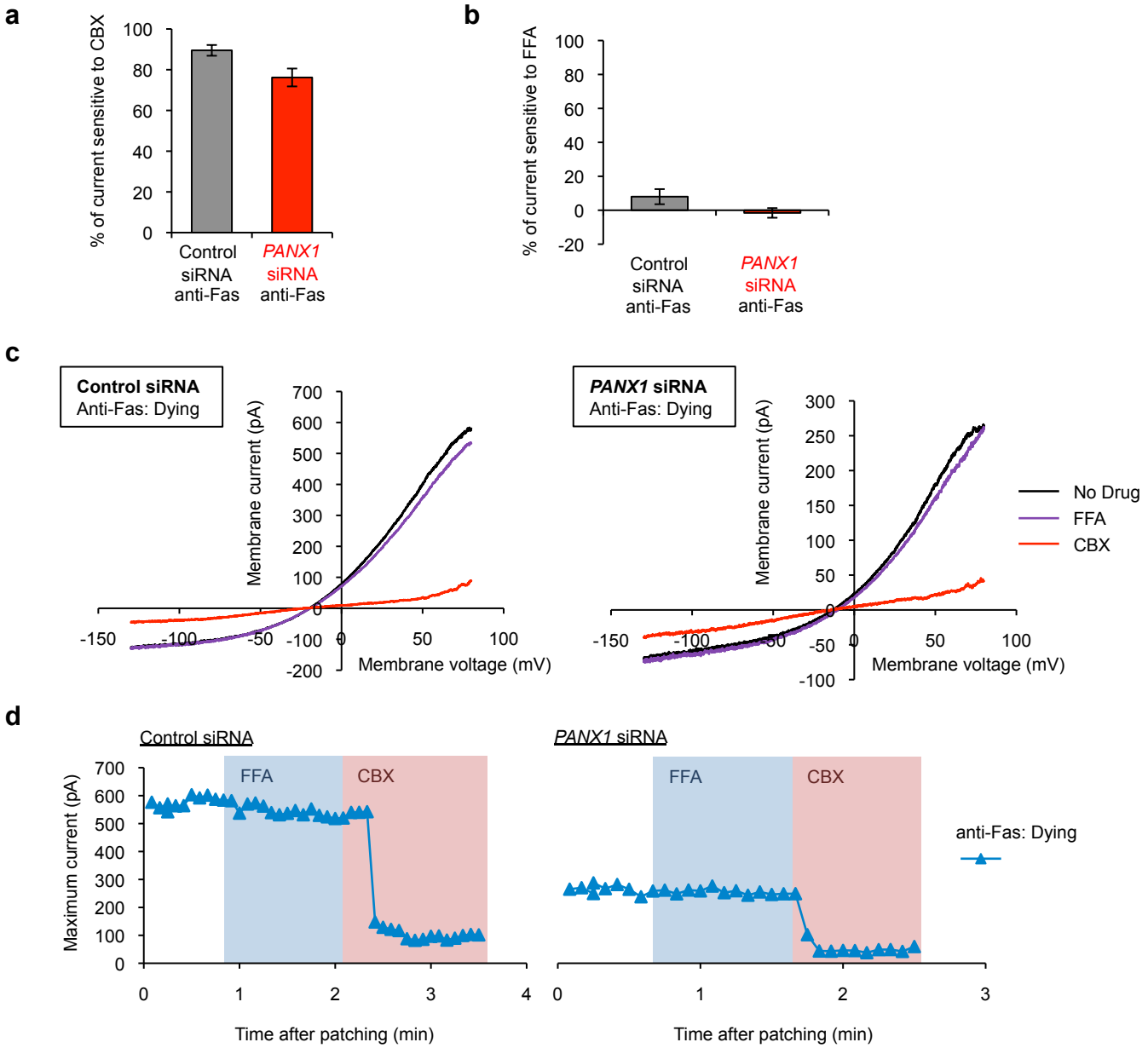

Supplementary Figure 8. Knockdown of pannexin 1 reduces the magnitude of the apoptosis-induced plasma membrane currents without affecting other properties.
Percentage of total membrane current that is sensitive to 100μM CBX (**a**) or 100μM FFA (**b**) in control- and *PANX1*-siRNA-transfected cells. Only cells receiving anti-Fas treatment that were dying were selected. $n \geq 8$ for each group. **c,** Current-voltage (I-V) relationships of apoptosis-induced current in anti-Fas treated dying Jurkat cells in control bath solution, or bath solution containing 100μM FFA or 100μM CBX. Membrane current was measured in a patched cell (only dying cells under anti-Fas treatment are shown here, since live cells have very little current) over a range of voltages, before and during perfusion of indicated drugs. While the shape of the I-V curves appear similar, please note the different scales on *y* axes. Exemplar records are representative of 8-11 cells. **d,** Patch-clamp recordings from dying siRNA-transfected Jurkat cells induced to undergo apoptosis with anti-Fas. Peak whole-cell current (at +90mV) is shown under conditions when bath solution was perfused with FFA (100μM, blue shading) or CBX (100μM, pink shading). Exemplar traces are representative of 8-11 cells. All error bars represent s.e.m.

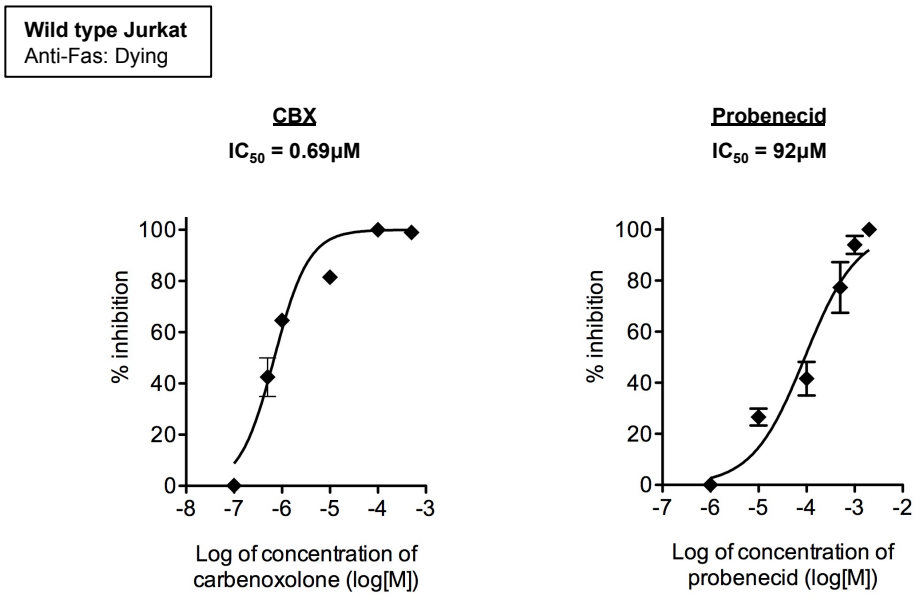

Supplementary Figure 9. Apoptosis-induced currents in wild-type Jurkat are sensitive to carbenoxolone and probenecid.
Dose response curves for pannexin 1 inhibitors carbenoxolone and probenecid on apoptosis-induced currents in Jurkat cells; data were normalized to inhibition at 0.1 and 1mM for CBX and probenecid, respectively. (Left) Dose response curves produced for CBX. *n* for each concentration of CBX are in parentheses: 500µM (3), 100µM (6), 10µM (6), 1µM (5), 500nM (6), 100nM (6). (Right) Dose response curves produced for probenecid. *n* = 5 for each of the following concentrations: 2mM, 1mM, 500µM, 100µM, 10µM, 1µM. Error bars, s.e.m.

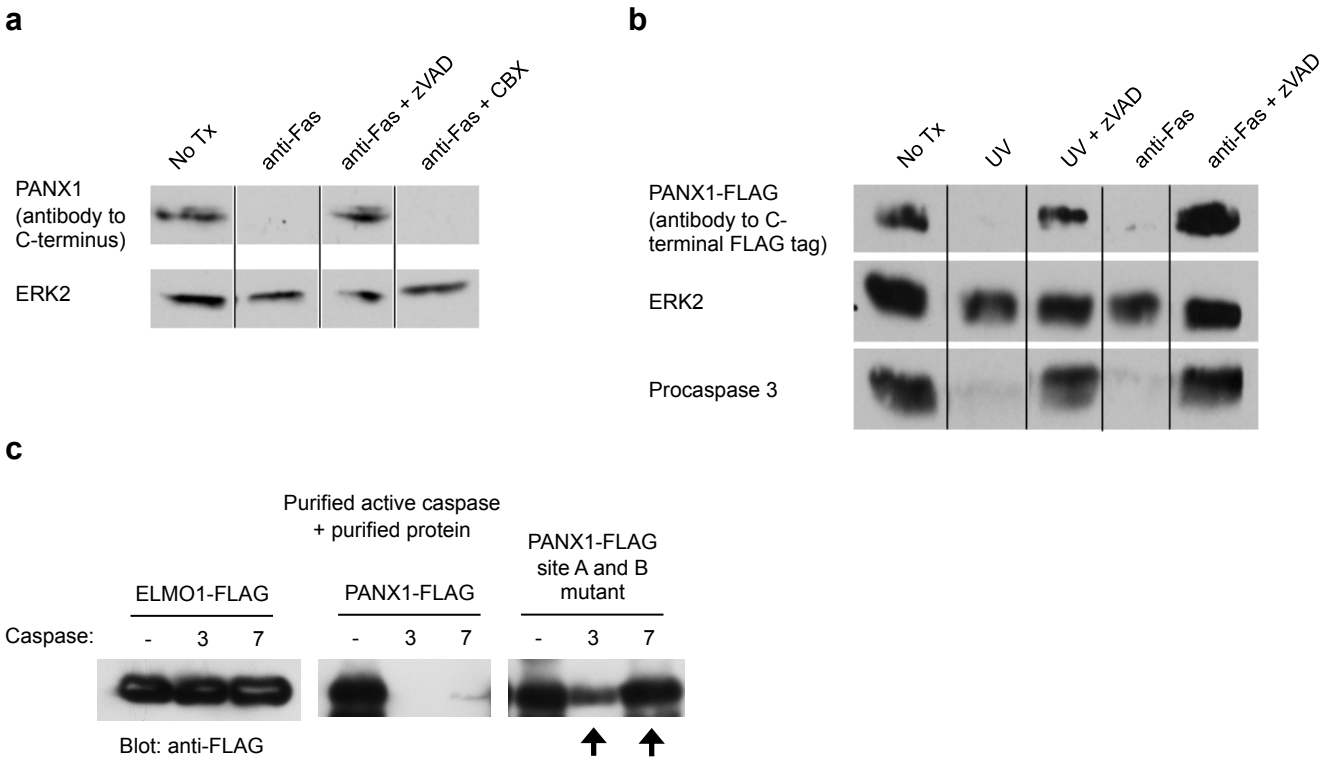

Supplementary Figure 10. Pannexin 1 is a target of caspase cleavage during apoptosis. **a**, Caspase inhibitor zVAD (50μM), but not CBX (500μM), restores PANX1 detection. Detection of endogenous PANX1 was assessed (using an antibody directed to the C-terminus of PANX1) in lysates of Jurkat cells induced to undergo Fas-mediated apoptosis. The level of ERK2 shows comparable loading of lysates in the different lanes. Please note that addition of the caspase inhibitor zVAD 'restored' PANX1 detection, while treatment with CBX did not. **b,** Loss of PANX1 immunoreactivity, detected with anti FLAG. Jurkat cells stably transfected with PANX1-FLAG were induced to undergo Fas- or UV-mediated apoptosis. Lysates of these cells were collected 2h post-induction, and PANX1 was detected with anti-FLAG immunoblotting. The levels of ERK2 revealed comparable loading of lysates in the different lanes. Immunoblotting for the cleavage of procaspase 3 was used a marker for induction of apoptosis. The addition of the caspase inhibitor zVAD (100μM) blocked procaspase 3 cleavage, and also 'restored' PANX1 detection. **c,** *In vitro* cleavage of immunoprecipitated ELMO1-FLAG, wild type PANX1-FLAG, and a mutant of PANX1 where both of the caspase cleavage (sites A and B) were disrupted (double mutant). ELMO1 and PANX1 proteins were expressed and purified, and then incubated with purified active caspases for 1h at 37°C. Loss of immunoreactivity to the antibody targeted to the C-terminal FLAG-tag of PANX1-FLAG (seen with caspases 3 and 7) was scored as caspase activity toward PANX1. Diminished or lack of cleavage of the PANX1 double mutant (for caspase 3 and 7, respectively), is indicated by arrows.

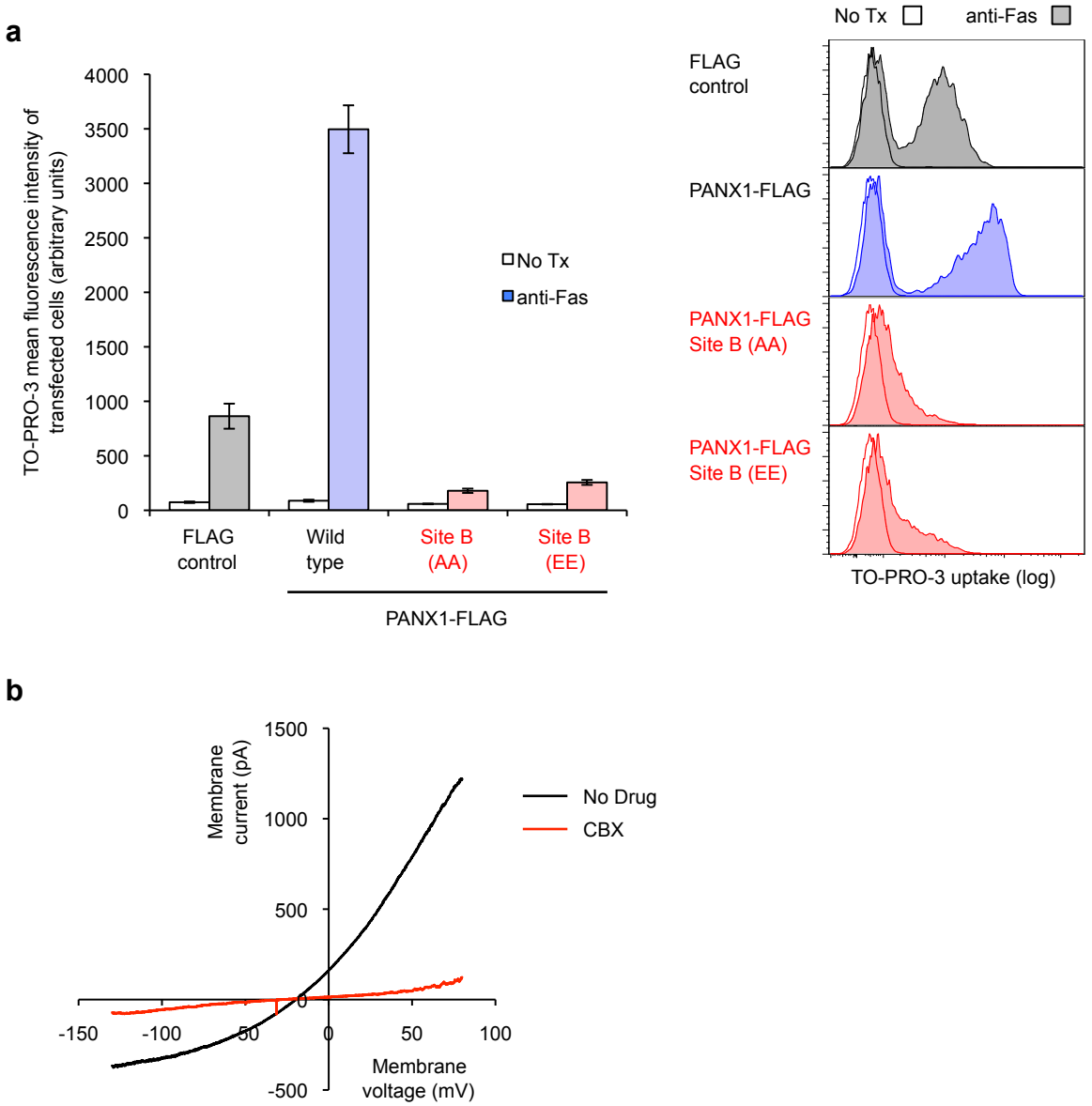

Supplementary Figure 11. Cleavage of pannexin 1 at site B results in channel permeability during apoptosis.

a, Disruption of site B in PANX1 by mutation of aspartic acid residues to either alanine (AA mutant) or glutamic acid (EE mutant) residues results in abrogated dye uptake during apoptosis. Jurkat cells were transiently co-transfected with plasmids coding for the indicated PANX1 proteins (wild type and site B mutants) and the fluorescent protein mBlueberry2 (as a marker for transfected cells). Cells were induced to undergo apoptosis by anti-Fas treatment and the transfected cells (gated based on mBlueberry2 expression) were assessed for TO-PRO-3 uptake by flow cytometry. (Left) The mean fluorescence intensity (MFI) for TO-PRO-3 uptake is displayed for the entire population of transfected cells. (Right) Flow cytometry histograms show dye uptake by apoptotic cells. Error bars, s.e.m.; *n* = 3.
b, Current-voltage (I-V) relationship of cell transiently transfected with PANX1 truncation mutant in control bath solution or bath solution containing 100μM CBX. Membrane current was measured in a patched cell (not induced to undergo apoptosis) over a range of voltages, before and during perfusion of CBX. While the shape of the I-V curves appear similar, please note the different scales on *y* axes. Exemplar records are representative of 7 cells.